



Published in final edited form as:

Mol Pharm. 2014 February 3; 11(2): 436–444. doi:10.1021/mp400396k.

Predicting the Outer Boundaries of P-glycoprotein (P-gp)-Based Drug Interactions at the Human Blood-Brain Barrier Based on Rat Studies

Peng Hsiao and Jashvant D Unadkat

Department of Pharmaceutics, University of Washington, Seattle, WA 98195

Abstract

Using positron emission tomography (PET), ^{11}C -verapamil as the P-gp substrate and cyclosporine A (CsA) as the P-gp inhibitor, we showed that the magnitude of P-gp-based drug interactions at the human blood-brain barrier (BBB) is modest. However, such interactions at clinically relevant CsA blood concentrations may be greater for substrates where P-gp plays an even larger role (fractional contribution of P-gp, $f_t > 0.97$) in preventing the CNS entry of the drug (e.g. nelfinavir). Since we have shown that the rat is an excellent predictor of the verapamil-CsA interaction at the human BBB, we determined the magnitude of drug interaction at the rat BBB between nelfinavir and CsA. Under isoflurane anesthesia, male Sprague Dawley rats were co-administered IV infusions of nelfinavir and escalating doses of CsA to achieve pseudo steady-state plasma/blood and brain concentrations of both drugs (blood CsA ranged 0–264.9 μM , $n=3-6$ /group). The percent increase in the brain:blood nelfinavir concentration ratio (determined by LC/MS) was described by the Hill equation with E_{max} 6481%, EC_{50} 12.3 μM , and γ 1.6. Then, using these data, as well as *in vitro* data in LLC PK1 cells expressing the human P-gp, we predicted that CsA (at clinically relevant blood concentration of 1.5 μM) will increase the distribution of nelfinavir into the human brain by 236%. Collectively, our data suggest that clinically significant P-gp based drug interactions at the human BBB are possible for P-gp substrates highly excluded from the brain ($f_t > 0.97$) and should be investigated using non-invasive approaches (e.g. PET).

Keywords

P-glycoprotein; blood-brain-barrier; drug-interaction; *in-vitro* to *in-vivo* correlation; rat model prediction to human clinical; fractional contribution of transporters; Cyclosporine A; Nelfinavir; positron emission tomography

INTRODUCTION

The blood brain barrier (BBB) poses a significant barrier to entry of drugs into the brain. An important component of this barrier is P-glycoprotein (P-gp), an ABC efflux pump that is expressed at the luminal membrane of the brain endothelial cells¹. Numerous studies in

small animals (e.g. mice or rat), either through ablation of the gene encoding P-gp (*mdr1a/b(-/-)*) or chemical inhibition of P-gp have demonstrated the importance of P-gp in preventing the entry of drugs into the brain. For example, the brain distribution of verapamil, nelfinavir or loperamide is increased by 800%, 3400% and 1200% respectively in *mdr1a/b(-/-)* vs. wild-type mice^{1; 2; 3}. When P-gp is chemically inhibited, in the mouse or the rat, the increase in brain distribution of these drugs is very similar; 900%, 3600% or 1500% increase in the presence vs. absence of the inhibitor^{2; 4; 5}.

Based on the above data, there are significant concerns (including in the drug development process) about large and clinically significant drug interactions at the human BBB. These concerns were somewhat allayed when the results from our ¹¹C-verapamil-cyclosporineA (CsA) study were published^{6; 7}. Using [¹¹C]-verapamil as a model P-gp substrate, at 3 μ M steady-state blood concentration, CsA (a P-gp inhibitor) increased the distribution of ¹¹C-verapamil into the human brain by a modest ~80%^{6; 7}. While such a magnitude of drug interaction at the human BBB could be significant for a narrow therapeutic window drug, it would be insignificant for the vast majority of drugs targeted to the CNS. Thus, these data pose another key question. Is the magnitude of drug interaction observed with ¹¹C-verapamil-CsA predictive of all possible P-gp based drug interaction at the human BBB? Obviously such extrapolation based on only one P-gp substrate-inhibitor combination is scientifically not justified. This is especially true for P-gp because it demonstrates allosterism and multiple binding sites^{8; 9; 10; 11; 12; 13}. Moreover, even in the absence of allosterism, if the P-gp drug substrate has a greater affinity for P-gp than verapamil and P-gp plays a larger role in preventing its entry into the CNS (e.g. nelfinavir), the extent of its drug interaction at the BBB with CsA would be expected to be even greater than that observed with verapamil³. Using the analogy of f_m (fraction of drug metabolized through a metabolic pathway), we refer to such substrates as those with large f_t . f_t represents the fractional contribution of a particular pathway, be it transport or diffusion of drug distribution into or out of a tissue. When f_t by P-gp at the BBB is greater than 0.97, even partial inhibition of P-gp (most probable in the clinic) will likely result in a significant drug interaction. Based on concerns of such drug interactions and exclusion from the brain, the pharmaceutical industry currently avoids development of CNS drugs that are P-gp substrates. Since conducting studies to determine drug interaction at the human BBB is challenging and requires non-invasive techniques such as imaging, predicting the theoretical outer boundary of P-gp based drug interactions at the human BBB would be enormously helpful in the drug development process. To predict this boundary, here we postulate that the largest such drug interaction will occur with a P-gp substrate that has an $f_t > 0.97$. The value of 0.97 was chosen for the simple reason that none of the approved drugs on the market are extremely potent inhibitors of P-gp at their unbound therapeutic plasma concentrations. Thus, in order for them to produce clinically significant drug interaction at the human BBB (e.g. with CsA), the f_t of a P-gp substrate will have to be >0.97) (see Discussion for details). On surveying the literature, nelfinavir appears to be such a drug. Nelfinavir has one of the largest increase in brain: blood concentration ratio in *mdr1a/b(-/-)* vs. wild-type mice (3400% increase, versus 900% for verapamil)^{3; 5}. Consistent with this observation, in non-human primates, we observed a 14500% increase in the brain distribution of nelfinavir in the presence of the selective and potent P-gp inhibitor, LY335979¹⁴.

We have previously demonstrated that the rat is an excellent animal model to predict the verapamil-CsA and loperamide-CsA drug interactions at the human BBB^{6; 15; 16; 17; 18}). Therefore, to predict the theoretical outer boundary of P-gp based drug interactions at the human BBB, we determined the magnitude of nelfinavir-CsA interaction at the rat BBB. Then, using these data and those from an *in vitro* LLCPK1-MDR1 cell assay, we predicted the maximum magnitude of nelfinavir-CsA interaction at the human BBB at clinically relevant blood CsA concentration. In addition, we provide a theoretical framework and provide guidelines of when and how to predict clinical significant drug interaction at the human BBB.

METHODS

Materials

[³H]-(+/-) Nelfinavir mesylate (3 Ci/mmol, [³H]-NFV) was purchased from American Radiolabeled Chemicals (St Louis, MO). Cyclosporine A (Sandimmune, 50 mg/mL) was purchased from Abbott Lab, Chicago, IL. Nelfinavir mesylate (NFV, formulated as 50 mg/mL in 650 mg Cremophore® EL and 32.9% ethanol by volume) was kind gift from Pfizer Inc.. All other reagents were of the highest grade available from commercial sources.

Animals

Male Sprague Dawley rats (8–10 wks, ~300g) were purchased from Taconic Farms. (Hudson, NY) and housed in a temperature and humidity controlled room with a 12-h light/dark cycle, with free access to food and water. The experimental protocol was approved by the Institutional Animal Care and Use Committee of the University of Washington. All experimental procedures were conducted according to the Guide for the Care and Use of Laboratory Animals (Institute of Laboratory Animal Resources, Commission on Life Sciences, National Research Council, Washington, DC, 1996).

Experimental protocol

Under isoflurane anesthesia (5% induction, 1–1.5% maintenance at 1.0 L/min), each animal was cannulated in both the left or right femoral artery and vein. Anesthesia was maintained throughout the experiment. The anesthesia plane and the condition of the animal were evaluated by routine tail/toe pinching test, respiration rate, and the palpebral reflex test. CsA (or vehicle) (0, 3.0, 4.5, 6.5, 9.0, 13.0, 16.2, 19.5 or 43.8 mg/kg in 0.1 mL) and NFV (1 mg/kg in 0.1 mL) were administered as an i.v. bolus, followed by a constant rate i.v. infusion of CsA plus NFV (0, 5.4, 9.0, 13.0, 18.0, 25.2, 32.4, 39.0 or 86.6 mg/kg/h CsA plus 1.2 mg NFV/kg/h at the rate of 0.5 mL/h) via the femoral vein to achieve pseudo steady-state blood CsA concentration of 0, 2.7 (3.3), 4.2 (5.0), 6.0 (7.2), 8.3 (10), 12.0 (14.4), 15.0 (18.0), 18 (21.7), 39.9 (48) μM, (μg/mL) respectively. CsA blood samples (~0.5 mL) were collected in heparanized tubes via the femoral artery at 0 (pre-CsA), 30, 60, 80, 100, and 120 min. Hematocrit in each blood sample (~50 μL) was determined immediately following each blood draw. Immediately following the 120 min blood draw, the animal was sacrificed by decapitation and the brain harvested. This time point was chosen based on reported NFV pharmacokinetic study in rats^{19; 20; 21; 22; 23} along with our pilot study in rats. Collectively, the literature and our pilot study results indicated that such duration was adequate for NFV

to reach pseudoequilibrium between the brain and plasma. Blood CsA concentrations were determined by LC/MS (Laboratory of Medicine at UWMC), while the brain, and plasma samples were stored at -20°C until analysis for NFV concentration by LC/MS.

Plasma and brain tissue analysis

Brain sample (0.4– 0.7 g) was homogenized, with PBS (100 μL PBS per 100 mg brain). The brain/PBS homogenates (100 μL) were then processed and analyzed by LC/MS as described below. The plasma and brain homogenate (100 μL) samples were precipitated with 1:1 acetonitrile containing 500 ng/mL of saquinavir (internal standard), followed by centrifugation at 20,800 g. The supernatant was then injected (5– 35 μl) onto an Agilent XDB-C18 reverse phase column (2.1 \times 50 mm, 5 μm , with Agilent XDB-C18 guard column, 2.1 \times 12.5 mm, 5 μm ; Agilent Technologies, Santa Clara, CA) eluted at 0.25 mL/min with a gradient mobile phase consisting of mobile phase A, 0.1% acetic acid in water, and mobile phase B, 1:1 of methanol: acetonitrile). The gradient was adjusted linearly as follows: 60% A/40% B for the first 0.5 min, 10% A/90% B from 0.5 to 2.5 min, maintained at 10% A/90% B from 2.5 to 3.5 min, 60% A/40% B from 3.5 min to 3.75 min, and maintained at this composition from 3.75 to 8.0 min. The mass spectrometer was operated in atmospheric pressure-ionization-electro-spray (API-ES) mode (spray chamber: gas temp 350°C , Vcap (+) 3500 V). Calibrators (1953 – 2 ng/ml) in plasma and quality control samples in plasma (1560, 98, 24, 8 ng/ml) and in brain homogenates (1560, 98, 24, 8 ng/ml) were analyzed in the same run. The limit of detection for nelfinavir in our tissue and plasma samples for this assay was 1 ng/g or 1 ng/mL respectively.

When pseudo steady-state blood (CsA) or plasma (NFV) concentrations of CsA or NFV were achieved, the average of these concentrations was computed and used. When CsA or NFV blood or plasma concentrations were not at pseudo steady-state, the average of the concentrations at the two last points were used. The brain: plasma ratio of NFV was adjusted for vascular contamination. We previously found that the brain vascular volume in the rat is $26.3 \pm 10 \mu\text{L/g}^{16}$. The blood: plasma ratio for NFV is 0.877²⁴. Using these values as well as the hematocrit values determined in our study, we estimated the vascular content of NFV in each brain sample. Then, the brain NFV concentration for each animal was corrected for the corresponding contamination from the vascular NFV content: $\text{brain}_{\text{corrected}} \text{NFV (ng/g)} = \text{brain}_{\text{uncorrected}} \text{NFV (ng/g)} - \text{plasma NFV (ng/1000}\mu\text{L)} \times \text{vascular volume } (\mu\text{L/g}) \times 0.877$. Using nonlinear regression (WinNonlin®; Pharsight Corporation), the Hill equation was fitted to the percent increase in the brain: plasma ratio of NFV as a function of blood CsA concentration. Unless otherwise stated, data are presented as mean \pm S.D. Analysis of variance, followed by Student's t-test was used to determine the statistical significance of difference ($p < 0.05$) between experimental groups.

Cell Culture

LLCPK1 cells transfected with MDR1¹⁵ were grown in complete media consisting of RPMI 1640 medium supplemented with 10% (v/v) fetal calf serum and 1% (v/v) antibiotic-antimycotic and grown at 37°C in the presence of 5% CO_2 .

[³H]-NFV Accumulation Assay

LLCPK1-transfected cells were plated at a density of 1×10^6 cells/well (1 mL/well, 1×10^6 cells/mL) on a 24-well plate, incubated at 37°C, 5% CO₂ overnight. For the accumulation of [³H]-NFV, the cells were washed with PBS followed by incubation (in quadruplicate) for 3 h in 1 mL serum free media at 37°C incubator in the presence of 5% CO₂ containing 30 nCi/mL (0.012 nM) [³H]-NFV, 0.2% dimethyl sulfoxide (DMSO) and varying concentration of CsA (0, 0.3, 1.0, 3.0 and 13.3 μM). After washing with 2 mL PBS, the cells in each well were lysed with 600 μL 1N NaOH, follow by addition of 600 μL 1N HCL to neutralize the solution. The intracellular accumulation of [³H]-NFV in each well (1000 μL of the lysate) was counted using scintillation counter. Protein content of each well was quantified by BCA assay and the intracellular accumulation of [³H]-NFV in each well was normalized for protein content.

The percent change in intracellular [³H]-NFV at each CsA concentration was expressed relative to that observed in the absence of the CsA. Using nonlinear regression (WinNonlin®; Pharsight Corporation), the Hill equation was fitted to the percent change in intracellular [³H]-NFV as a function of increasing CsA concentration. The mean EC₅₀ of each CsA was determined from 3 or more independent experiments. Unless otherwise stated, data are presented as mean ± S.D.

RESULTS

***In vivo* Study**

Except at the higher CsA infusion rates, the targeted pseudo steady-state blood CsA concentrations were achieved prior to the experimental end point (120 min). These concentrations were 3.0 ± 0.2 (n=3), 4.0 ± 0.5 (n=3), 6.7 ± 0.8 (n=3), 11.9 ± 1.3 (n=4), 20.3 ± 1.2 (n=3), 33.1 ± 4.7 (n=5), 96.3 ± 37.5 (n=3), and 264.9 ± 58.9 (n=3) μM CsA at infusion rate of 5.4, 9.0, 13.0, 18.0, 25.2, 32.4, 39.0 and 86.6 mg/kg/h, respectively (Fig. 1). The higher than targeted blood CsA concentrations achieved at the higher CsA infusion rates (32, 39 and 86.6 mg/kg/hr) were most likely due to nonlinearity in the pharmacokinetics of CsA.

Targeted pseudo steady-state plasma NFV concentration were also achieved and maintained during the duration of the experiment (Fig. 2A). The presence of CsA did not significantly affect the pseudo steady-state plasma NFV concentration (Student's t-test) at the experimental end point (120 min) (Fig. 2B).

In the absence of CsA, the NFV brain:plasma concentration was low (0.044 ± 0.01 , n=6). This ratio decreased dramatically to 0.014 ± 0.01 (n=6) when corrected for vascular contamination. With increasing CsA blood concentration, the corrected NFV brain:plasma concentration ratio increased significantly to 0.097 ± 0.04 (n=3), 0.167 ± 0.02 (n=3), 0.255 ± 0.06 (n=3), 0.389 ± 0.12 (n=4), 0.638 ± 0.08 (n=3), 0.804 ± 0.07 (n=5), 0.769 ± 0.23 (n=3), and 0.899 ± 0.16 (n=3) for blood CsA concentration of 3.0, 4.0, 6.7, 11.9, 20.3, 33.1, 96.4 and 264.9 μM, respectively. The percent increase in the brain:plasma NFV concentration ratio, expressed relative to that in the control group (absence of CsA), increased as the blood CsA concentration increased (Fig. 3). The Hill equation (Fig. 3) was

fitted to these data using nonlinear regression (uniform weighting) and yielded the following estimates (% CV of the estimate): E_{\max} 6481% (5.9%), EC_{50} 12.3 μM (13.5%), and γ 1.6 (16.5%).

Impact of vascular contamination on estimation of brain:plasma ratio of P-gp substrates

We conducted simulations to explore the impact of vascular content correction (as described above for NFV) on the brain:plasma concentration of P-gp substrates (Fig 4). First, we computed the percent difference in brain:plasma drug concentration ratio at maximal P-gp inhibition when this value is corrected vs. uncorrected for vascular content. Then, we plotted this value, in 3D, with respect to brain: plasma of the drug in the absence (i.e. at baseline) and presence of maximal P-gp inhibition, both corrected for vascular content (Y and X axis respectively). As expected, the impact of this correction was largest for drugs that had high $f_{t(\text{P-gp})}$ value (i.e. low brain penetration) at baseline.

In vitro Study

Based on three independent *in vitro* LLCPK1-MDR1 accumulation assays (Fig. 5 shows a representative experiment), the *in vitro* E_{\max} , EC_{50} , and γ of CsA was determined to be $205 \pm 10\%$, $1.3 \pm 0.5 \mu\text{M}$, and 1.4 ± 0.4 , respectively.

Prediction of *in vivo* NFV-CsA drug interaction at the human BBB based on the rat and *in vitro* cell culture study

As described before¹⁵, the above *in vitro* data were scaled using the *in vivo* data in the rat to predict the magnitude of P-gp NFV-CsA interaction at the human BBB at clinically relevant and supratherapeutic CsA blood concentrations. At supratherapeutic CsA blood concentration (achieved in our prior human PET study, 2.8 μM), we predicted a 555% increase in the NFV brain: plasma concentration ratio. This is significantly greater than the modest 75 and 79% increase we observed in the rat and human brain when verapamil was used as a substrate^{6; 16}. At therapeutic CsA blood concentration (1.5 μM), we predicted a 241% increase in the NFV brain:plasma concentration ratio. These predicted values were comparable to the 589% (2.8 μM) and 236% (1.5 μM) increase in NFV human brain:plasma concentration ratio when the predictions were based on the rat study alone (Fig. 3).

Impact of $f_{t(\text{P-gp})}$ on magnitude of P-gp inhibition

To illustrate the impact of $f_{t(\text{P-gp})}$ on P-gp inhibition at the BBB, we simulated and plotted the percent increase in brain:plasma drug concentration ratio for drugs with different $f_{t(\text{P-gp})}$ values in the absence and presence of P-gp inhibition (Fig 6A). P-gp inhibition was varied from that expected at clinical CsA blood concentrations (3.3% P-gp inhibition) to when P-gp was completely inhibited. The derivation of equations used to conduct these simulations have been published elsewhere^{25; 26; 27; 28} and the final equations used are shown on Fig. 6B. These equations are predicated on the assumption that nonspecific binding of NFV to brain tissue is non-saturable. As expected, as $f_{t(\text{P-gp})}$ increased, P-gp inhibition (including at clinical CsA blood concentration) drastically increased the percent increase in brain: plasma ratio of the drug. In addition, when a drug was efficiently excluded from the brain by P-gp (low brain penetration; $f_{t(\text{P-gp})} > 0.97$), if vascular content correction was not made, the

increase in brain: plasma ratio of the P-gp substrate, on complete inhibition of P-gp, was considerably underestimated. To further illustrate the impact of P-gp inhibition on brain drug penetration, we plotted the latter with respect to percent P-gp inhibition (Fig. 6B). Reminiscent of the impact of f_m (fraction of drug metabolized by a single pathway) on metabolic drug interactions, the % increase in brain: plasma ratio was profound for $f_{t(P-gp)} > 0.9$ when P-gp inhibition was greater than 90%. Furthermore, for P-gp drug substrates with $f_{t(P-gp)} > 0.95$, the increase in brain: plasma concentration ratio of the P-gp substrate, on complete inhibition of P-gp, was considerably underestimated (e.g. NFV), when this value was not corrected for vascular content.

DISCUSSION

f_t , represents the fractional contribution of a particular mechanism, be it transport or diffusion of a drug in the distribution into or out of a tissue. This term is useful for all transporter-mediated drug interactions. For example, if f_t via an influx transporter (e.g. OATP) is responsible for 0.9 of the entry of a drug into the liver, complete inhibition of this transporter will result in at least 10-fold increase in the systemic concentration of the drug provided the influx transporter (in the liver) is the sole route of elimination of the drug. Likewise, when f_t by P-gp efflux at the BBB is 0.97 for preventing the entry of the drug into the brain, even partial inhibition of P-gp (e.g. at clinical relevant CsA doses) will likely result in a significant drug interaction at the BBB. Since nelfinavir represents such a drug ($f_{t(P-gp)} \sim 0.98$; see below), it can be used as model P-gp drug to investigate the maximum potential of P-gp based drug interactions at the rat BBB and, by extrapolation from these rat studies and *in vitro* studies in LLCPK-MDR1 cells, the maximum potential of P-gp based drug interaction at the human BBB. This manuscript presents results from such studies.

Unlike verapamil, correction of brain nelfinavir concentration for vascular content substantially changed the brain: plasma concentration ratio of NFV from 0.044 without correction to 0.014 with correction. This notable difference was due to the brain concentrations of nelfinavir being much lower than the corresponding plasma concentrations due to greater P-gp mediated efflux of nelfinavir and the high percentage of NFV bound to plasma proteins. In rodents, the percent of NFV bound to plasma proteins is 99.9% while that for verapamil is 89% (0.1% and 11% unbound, respectively,²⁹). For low brain penetrating P-gp substrate drugs (where the uncorrected brain: plasma ratio in the absence of P-gp inhibition is low), on inhibition of P-gp, the % increase in brain: plasma ratio can change drastically when corrected for vascular content (Fig. 4). When such correction is not made (as is often the case), the contribution of P-gp with the distribution of the P-gp substrate drug into the brain will be considerably underestimated. As in the case of NFV in this study, at 246.9 μ M CsA blood concentration, we reported a 2110% increase in NFV brain: blood ratio without vascular content correction versus 6420% increase when the correction was made (Fig. 4).

As P-gp activity was inhibited by increasing blood CsA concentration, the NFV brain: plasma ratios, after vascular-content correction (0.90 ± 0.16) became similar to the uncorrected value (0.93 ± 0.16). Using the vascular-content corrected NFV brain: plasma ratio of 0.014 and 0.90 for without and with maximum P-gp inhibition, the fraction of P-gp

contribution ($f_{t(P-gp)}$) in preventing NFV brain distribution was estimated to be 0.984 ((0.9 – 0.014)/0.9). When the brain:plasma ratio was not corrected for vascular content (as is often the case), the $f_{t(P-gp)}$ was considerably underestimated to be 0.95 (((0.93 – 0.044)/0.93), Fig. 6A). In contrast to NFV, the difference between vascular content corrected and uncorrected $f_{t(P-gp)}$ for verapamil is quite small (0.962 and 0.960 for corrected and uncorrected $f_{t(P-gp)}$, respectively; blood to plasma partition coefficient of verapamil is 0.75–0.96^{6; 16; 30}), and thus correction of brain verapamil concentration for vascular content is not necessary. As $f_{t(P-gp)}$ increases to >0.97, when the difference between vascular content corrected and uncorrected $f_{t(P-gp)}$ is 0.03 or greater, then the % increase in brain: plasma ratio of the drug, on inhibiting P-gp, increases dramatically (Fig. 6A). Such relationship of exposure to inhibition of efflux has been examined previously at the level of liver and the term f_e was introduced as the fraction of total clearance mediated by the transporter involved²⁸. This phenomenon is comparable to the dependence of the magnitude of drug interaction on f_m (fraction of a dose metabolized via a pathway). As f_m approaches unity, the magnitude of change in AUC of a drug can be profound when this pathway is significantly inhibited^{25; 26; 27}. To illustrate this point, a similar plot can be constructed for percent increase in brain: plasma ratio due to P-gp inhibition using $f_{t(P-gp)}$, and percent P-gp inhibition (Fig 6B). However, this plot can also be used for any transporter-based drug interactions.

We have previously shown that at the same blood concentrations of CsA as those achieved in humans (2.8 and 5.6 μM), P-gp inhibition at the rat and human BBB is quantitatively similar (75% vs.79% increase in total verapamil-radioactivity uptake into the brain of rats and humans at 2.8 μM CsA blood concentration, respectively^{6; 16} and 588% vs.522% increase in total loperamide-radioactivity uptake into the brain of rats and humans at 5.6 μM CsA blood concentration, respectively^{17; 18}. Based on these data we concluded that the rat is an excellent predictor of P-gp based interactions at the human BBB (our *in vitro* data support this assertion – see below). At CsA blood concentration of 2.8 μM , the percent increase in nelfinavir rat brain: plasma concentration ratio was estimated to be 598%. This is significantly greater than the modest 75% increase observed when verapamil was used as a substrate. Based on the rat data as well as the *in vitro* cell culture data, we predict a similar 555% increase in the concentration of NFV in human brain in the presence of 2.8 μM CsA. At clinically relevant blood concentration of CsA (1.5 μM), we predict a 241% increase in the distribution of NFV into the human brain.

The above data suggest that the magnitude of P-gp based drug interactions at the BBB, for P-gp substrates with narrow therapeutic window and significantly excluded from the brain ($f_{t(P-gp)} > 0.97$), can be clinically significant and much greater than that observed for verapamil-CsA interaction, even at therapeutically relevant CsA blood concentration. This prediction will need to be tested in humans (with either PET-labeled NFV or another PET-labeled high affinity P-gp substrate). With 2.33-fold lower P-gp expression in human versus mice³¹, one could postulate that P-gp substrate drugs may be less well excluded from the human vs. the rodent brain (lower f_t via the P-gp pathway in humans). Consequently, this large magnitude of interactions observed in rodents may be reduced in humans. Even so, evidence in the literature suggest that the magnitude of P-gp drug interaction at the human

BBB can indeed be much greater than that observed with [^{11}C]-verapamil-CsA. For example, using tariquidar (XR9576), a potent third generation investigational P-gp inhibitor³², and [^{11}C]-N-desmethyl-loperamide ([^{11}C]dLop,³³) as the P-gp substrate, Kreisl et al., showed that tariquidar (6 mg/kg) could increase the distribution of [^{11}C]dLop into the human brain by as much as 300%³⁴. Based on animal data, the $f_{i(\text{P-gp})}$ for dLop appears to be a lower than that for NFV. In the P-gp-knock-out mice the brain: blood concentration ratio of NFV, dLop and verapamil, is 3400%, 1600% and 800% higher than the wild-type mice^{2; 3; 35}. Therefore, it is reasonable to propose that if tariquidar were to be co-administered with a drug like NFV, that the magnitude of interaction at the human BBB would be even greater than 300%. While a change of this magnitude in brain distribution of a drug would be of concern for inadvertent drug interactions, these data also suggest that P-gp inhibitors could be effectively used to increase the efficacy of drugs that are excluded from the CNS. For example, patients with primary brain tumor and brain metastasis have poor response to chemotherapy primarily due to impermeability of the BBB to cytotoxic agents. As shown in nude mice implanted with intracerebral human glioblastoma, overcoming the P-gp BBB by co-administration of the second generation P-gp inhibitor, PSC833, with paclitaxel, results in significant reduction in the brain tumor volume when compared to paclitaxel alone³⁶.

In development of a new molecular entity (NME) that is an excellent P-gp substrate/inhibitor, there is often a concern that it may produce P-gp-based inhibitory drug interactions at the human BBB or will be subject to such interactions. Based on the data presented here, to estimate the maximum liability of the NME to produce such interactions, we propose that NFV be used as a model substrate and the NME as an inhibitor at plasma concentrations likely to be achieved in humans. To address the reverse question, that is the maximum P-gp based drug interactions at the human BBB that the NME will be subjected to (e.g. when co-administered with CsA, one of the most potent P-gp inhibitor on the market) we propose that the $f_{i(\text{P-gp})}$ of the new molecular entity be determined in rodents where P-gp has been genetically or chemically knocked-out. Based on this $f_{i(\text{P-gp})}$, the maximum possible drug interaction at the human BBB of the NME with clinically relevant CsA blood concentrations (1.5 μM) can be estimated (Fig 6A).

In this study, when NFV was used as the P-gp substrate (NFV is not a substrate of BCRP,³⁷), the EC_{50} of CsA to inhibit P-gp at the rat BBB was significantly greater ($12.3 \pm 1.7 \mu\text{M}$) than that observed when verapamil or loperamide was used as a substrate ($7.2 \pm 0.5 \mu\text{M}$ and $7.1 \pm 0.6 \mu\text{M}$, respectively); the Hill coefficient when nelfinavir was used as a substrate (1.6 ± 0.3) was significantly lower than when verapamil or loperamide was used as a substrate (3.8 ± 0.9 and 3.7 ± 1.1 , respectively). Collectively, these data suggest that even when the same inhibitor (CsA) is used, its interaction with nelfinavir, verapamil or loperamide for P-gp transport appears to differ. Such differences allude to possible differences in the binding sites of verapamil and nelfinavir and perhaps allosteric behavior of P-gp but we cannot discount other mechanisms. Such allosteric behavior could result in much greater interaction at the BBB for one pair of inhibitor-substrate pair as opposed to another pair. The above data make it imperative that additional studies of drug interactions at the human BBB be conducted using ^{11}C -verapamil as a substrate and inhibitors other than CsA, or using CsA as the inhibitor and different ^{11}C -compounds as the P-gp substrates.

For this NFV study, the *in vitro* EC₅₀ of CsA from the LLCPK1-MDR1 cell line (1.3 ± 0.5 μ M) was consistent with the *in vivo* unbound EC₅₀ (0.9 ± 0.1 μ M) at the rat BBB (unbound EC₅₀ value was computed using the reported CsA fraction unbound of 7% in the rat (Bernareggi and Rowland, 1991)). This is consistent with the finding in our prior *in vitro- in vivo* correlation study using verapamil-CsA, and loperamide-CsA as the P-gp substrate pair (*in vitro* EC₅₀ of 0.6 ± 0.3 μ M vs. *in vivo* unbound EC₅₀ of 0.47 ± 0.004 μ M at the rat BBB¹⁵ and *in vitro* EC₅₀ of 0.78 ± 0.04 μ M vs. *in vivo* unbound EC₅₀ of 0.50 ± 0.04 μ M at the rat BBB^(38, 18, respectively)). The present data provide further support to the notion that inhibition of P-gp at the rat BBB is consistent with that observed with human P-gp expressed in LLCPK1-MDR1 cell line.

In conclusion, our drug interaction data in the rat suggest that P-gp based drug interactions at the human BBB can be clinically significant for P-gp substrates with a narrow therapeutic window that are highly excluded from the CNS by P-gp ($f_{t(P-gp)} > 0.97$). This is in agreement with the analysis of Kalvass et al³⁹. Studies with PET-labeled NFV or another high affinity P-gp substrate are needed to test this prediction. In addition, there is remarkable *in vitro* (LLCPK1-MDR1 cells) to *in vivo* (rat) correlation of the potency of CsA to inhibit P-gp. Studies with additional substrates and inhibitors are needed to confirm that the rat, together with *in vitro* studies in LLCPK1-MDR1 cells, can predict the magnitude of P-gp drug interactions at the human BBB. In the meantime, to estimate the maximum liability for P-gp-based drug interactions that a NME will produce (perpetrator), we propose that rodent studies be conducted with NFV as the substrate (with vascular content correction) and the NME as an inhibitor. To estimate the maximum liability for P-gp based drug interactions that a NME will be subjected to (victim), we propose that the $f_{t(P-gp)}$ of the NME be determined in rodents where P-gp has been genetically ablated or completely inhibited with selective P-gp inhibitors.

Acknowledgments

The authors are grateful to Dr. Rodney JY Ho, Department of Pharmaceutics, (University of Washington, Seattle, Washington) for providing the LLCPK1-MDR1 cell line for the *in vitro* experiments described in this paper, and to Li Liu for her insightful and critical discussion of this manuscript.

This work was supported by NCR Grant TL1 RR 025016, the ITHS TL1 Multidisciplinary Predoctoral Clinical Research Training Program (PHS2271) and NIH grants GM032165, and RCNS068404.

Abbreviations

P-gp	P-glycoprotein
BBB	blood-brain-barrier
CsA	Cyclosporine A
NFV	Nelfinavir
PET	positron emission tomography

REFERENCES

1. Schinkel AH, Wagenaar E, Mol CA, van Deemter L. P-glycoprotein in the blood-brain barrier of mice influences the brain penetration and pharmacological activity of many drugs. *J Clin Invest.* 1996; 97:2517–2524. [PubMed: 8647944]
2. Hendrikse NH, Schinkel AH, de Vries EG, Fluks E, Van der Graaf WT, Willemsen AT, Vaalburg W, Franssen EJ. Complete in vivo reversal of P-glycoprotein pump function in the blood-brain barrier visualized with positron emission tomography. *Br J Pharmacol.* 1998; 124:1413–1418. [PubMed: 9723952]
3. Kim RB, Fromm MF, Wandel C, Leake B, Wood AJ, Roden DM, Wilkinson GR. The drug transporter P-glycoprotein limits oral absorption and brain entry of HIV-1 protease inhibitors. *J Clin Invest.* 1998; 101:289–294. [PubMed: 9435299]
4. Choo EF, Kurnik D, Muszkat M, Ohkubo T, Shay SD, Higginbotham JN, Glaeser H, Kim RB, Wood AJ, Wilkinson GR. Differential in vivo sensitivity to inhibition of P-glycoprotein located in lymphocytes, testes, and the blood-brain barrier. *J Pharmacol Exp Ther.* 2006; 317:1012–1018. [PubMed: 16537797]
5. Choo EF, Leake B, Wandel C, Imamura H, Wood AJ, Wilkinson GR, Kim RB. Pharmacological inhibition of P-glycoprotein transport enhances the distribution of HIV-1 protease inhibitors into brain and testes. *Drug Metab Dispos.* 2000; 28:655–660. [PubMed: 10820137]
6. Sasongko L, Link JM, Muzi M, Mankoff DA, Yang X, Collier AC, Shoner SC, Unadkat JD. Imaging P-glycoprotein transport activity at the human blood-brain barrier with positron emission tomography. *Clin Pharmacol Ther.* 2005; 77:503–514. [PubMed: 15961982]
7. Eyal S, Ke B, Muzi M, Link JM, Mankoff DA, Collier AC, Unadkat JD. Regional P-glycoprotein activity and inhibition at the human blood-brain barrier as imaged by positron emission tomography. *Clin Pharmacol Ther.* 2010; 87:579–585. [PubMed: 20336065]
8. Aller SG, Yu J, Ward A, Weng Y, Chittaboina S, Zhuo R, Harrell PM, Trinh YT, Zhang Q, Urbatsch IL, Chang G. Structure of P-glycoprotein reveals a molecular basis for poly-specific drug binding. *Science.* 2009; 323:1718–1722. [PubMed: 19325113]
9. Martin C, Berridge G, Higgins CF, Mistry P, Charlton P, Callaghan R. Communication between multiple drug binding sites on P-glycoprotein. *Mol Pharmacol.* 2000; 58:624–632. [PubMed: 10953057]
10. Martin C, Berridge G, Mistry P, Higgins C, Charlton P, Callaghan R. The molecular interaction of the high affinity reversal agent XR9576 with P-glycoprotein. *Br J Pharmacol.* 1999; 128:403–411. [PubMed: 10510451]
11. Martin C, Berridge G, Mistry P, Higgins C, Charlton P, Callaghan R. Drug binding sites on P-glycoprotein are altered by ATP binding prior to nucleotide hydrolysis. *Biochemistry.* 2000; 39:11901–11906. [PubMed: 11009602]
12. Shapiro AB, Fox K, Lam P, Ling V. Stimulation of P-glycoprotein-mediated drug transport by prazosin and progesterone. Evidence for a third drug-binding site. *Eur J Biochem.* 1999; 259:841–850. [PubMed: 10092872]
13. Taub ME, Podila L, Ely D, Almeida I. Functional assessment of multiple P-glycoprotein (P-gp) probe substrates: influence of cell line and modulator concentration on P-gp activity. *Drug Metab Dispos.* 2005; 33:1679–1687. [PubMed: 16093365]
14. Kaddoumi A, Choi SU, Kinman L, Whittington D, Tsai CC, Ho RJ, Anderson BD, Unadkat JD. Inhibition of P-glycoprotein activity at the primate blood-brain barrier increases the distribution of nelfinavir into the brain but not into the cerebrospinal fluid. *Drug Metab Dispos.* 2007; 35:1459–1462. [PubMed: 17591677]
15. Hsiao P, Bui T, Ho RJ, Unadkat JD. In vitro-to-in vivo prediction of P-glycoprotein-based drug interactions at the human and rodent blood-brain barrier. *Drug Metab Dispos.* 2008; 36:481–484. [PubMed: 18057117]
16. Hsiao P, Sasongko L, Link JM, Mankoff DA, Muzi M, Collier AC, Unadkat JD. Verapamil P-glycoprotein transport across the rat blood-brain barrier: cyclosporine, a concentration inhibition analysis, and comparison with human data. *J Pharmacol Exp Ther.* 2006; 317:704–710. [PubMed: 16415090]

17. Passchier J, Comley R, Salinas C, Rabiner E, Gunn R, Cunningham V, Wilson A, Houle S, Gee A, Laruelle M. Blood brain barrier permeability of [¹¹C]loperamide in humans under normal and impaired P-glycoprotein function. *J NUCL MED MEETING ABSTRACTS*. 2008; 49 211P-.
18. Hsiao P, Unadkat JD. P-glycoprotein-based loperamide-cyclosporine drug interaction at the rat blood-brain barrier: prediction from in vitro studies and extrapolation to humans. *Mol Pharm*. 2012; 9:629–633. [PubMed: 22316009]
19. Shibata N, Gao W, Okamoto H, Kishida T, Yoshikawa Y, Takada K. In-vitro and in-vivo pharmacokinetic interactions of amprenavir, an HIV protease inhibitor, with other current HIV protease inhibitors in rats. *J Pharm Pharmacol*. 2002; 54:221–229. [PubMed: 11848286]
20. Anderson BD, May MJ, Jordan S, Song L, Roberts MJ, Leggas M. Dependence of nelfinavir brain uptake on dose and tissue concentrations of the selective P-glycoprotein inhibitor zosuquidar in rats. *Drug Metab Dispos*. 2006; 34:653–659. [PubMed: 16434546]
21. Kempf DJ, Marsh KC, Kumar G, Rodrigues AD, Denissen JF, McDonald E, Kukulka MJ, Hsu A, Granneman GR, Baroldi PA, Sun E, Pizzuti D, Plattner JJ, Norbeck DW, Leonard JM. Pharmacokinetic enhancement of inhibitors of the human immunodeficiency virus protease by coadministration with ritonavir. *Antimicrob Agents Chemother*. 1997; 41:654–660. [PubMed: 9056009]
22. Zhang KE, Wu E, Patick AK, Kerr B, Zorbas M, Lankford A, Kobayashi T, Maeda Y, Shetty B, Webber S. Circulating metabolites of the human immunodeficiency virus protease inhibitor nelfinavir in humans: structural identification, levels in plasma, and antiviral activities. *Antimicrob Agents Chemother*. 2001; 45:1086–1093. [PubMed: 11257019]
23. Shetty BV, Kosa MB, Khalil DA, Webber S. Preclinical pharmacokinetics and distribution to tissue of AG1343, an inhibitor of human immunodeficiency virus type 1 protease. *Antimicrob Agents Chemother*. 1996; 40:110–114. [PubMed: 8787890]
24. Sugioka N, Sato K, Haraya K, Maeda Y, Yasuda K, Fukushima K, Ito Y, Takada K. Effect of streptozotocin-induced diabetes mellitus on the pharmacokinetics of nelfinavir in rats. *Biopharm Drug Dispos*. 2008; 29:469–479. [PubMed: 19009515]
25. Boxenbaum H. Human in vivo competitive inhibition of P450 substrates: increased plasma concentrations as a function of hepatic extraction ratio and percent inhibition. *J Pharm Pharm Sci*. 1999; 2:89–91. [PubMed: 10953254]
26. Ito K, Hallifax D, Obach RS, Houston JB. Impact of parallel pathways of drug elimination and multiple cytochrome P450 involvement on drug-drug interactions: CYP2D6 paradigm. *Drug Metab Dispos*. 2005; 33:837–844. [PubMed: 15897600]
27. Rowland M, Matin SB. Kinetics of drug-drug interactins. *J Pharmacokinet Biopharm*. 1973; 1:553–567.
28. Zamek-Gliszczynski MJ, Kalvass JC, Pollack GM, Brouwer KL. Relationship between drug/metabolite exposure and impairment of excretory transport function. *Drug Metab Dispos*. 2009; 37:386–390. [PubMed: 19022942]
29. Kalvass JC, Maurer TS, Pollack GM. Use of plasma and brain unbound fractions to assess the extent of brain distribution of 34 drugs: comparison of unbound concentration ratios to in vivo p-glycoprotein efflux ratios. *Drug Metab Dispos*. 2007; 35:660–666. [PubMed: 17237155]
30. Manitpisitkul P, Chiou WL. Intravenous verapamil kinetics in rats: marked arteriovenous concentration difference and comparison with humans. *Biopharm Drug Dispos*. 1993; 14:555–566. [PubMed: 8251610]
31. Uchida Y, Ohtsuki S, Katsukura Y, Ikeda C, Suzuki T, Kamiie J, Terasaki T. Quantitative Targeted Absolute Proteomics of Human Blood-Brain Barrier Transporters and Receptors. *J Neurochem*. 2011
32. Mistry P, Stewart AJ, Dangerfield W, Okiji S, Liddle C, Bootle D, Plumb JA, Templeton D, Charlton P. In vitro and in vivo reversal of P-glycoprotein-mediated multidrug resistance by a novel potent modulator, XR9576. *Cancer Res*. 2001; 61:749–758. [PubMed: 11212278]
33. Lazarova N, Zoghbi SS, Hong J, Seneca N, Tuan E, Gladding RL, Liow JS, Taku A, Innis RB, Pike VW. Synthesis and evaluation of [N-methyl-¹¹C]N-desmethyl-loperamide as a new and improved PET radiotracer for imaging P-gp function. *J Med Chem*. 2008; 51:6034–6043. [PubMed: 18783208]

34. Kreisl WC, Liow JS, Kimura N, Seneca N, Zoghbi SS, Morse CL, Herscovitch P, Pike VW, Innis RB. P-glycoprotein function at the blood-brain barrier in humans can be quantified with the substrate radiotracer 11C-N-desmethyl-loperamide. *J Nucl Med.* 2010; 51:559–566. [PubMed: 20237038]
35. Zoghbi SS, Liow JS, Yasuno F, Hong J, Tuan E, Lazarova N, Gladding RL, Pike VW, Innis RB. 11C-loperamide and its N-desmethyl radiometabolite are avid substrates for brain permeability-glycoprotein efflux. *J Nucl Med.* 2008; 49:649–656. [PubMed: 18344435]
36. Fellner S, Bauer B, Miller DS, Schaffrik M, Fankhanel M, Spruss T, Bernhardt G, Graeff C, Farber L, Gschaidmeier H, Buschauer A, Fricker G. Transport of paclitaxel (Taxol) across the blood-brain barrier in vitro and in vivo. *J Clin Invest.* 2002; 110:1309–1318. [PubMed: 12417570]
37. Gupta A, Zhang Y, Unadkat JD, Mao Q. HIV protease inhibitors are inhibitors but not substrates of the human breast cancer resistance protein (BCRP/ABCG2). *J Pharmacol Exp Ther.* 2004; 310:334–341. [PubMed: 15007102]
38. Corkill G, Turner D, Pufong B, Gill H, Fessey R, Dilworth C. *In vitro* evaluation of P-glycoprotein inhibition using loperamide as a probe substrate. 10 th European ISSX Meeting. 2008
39. Kalvass JC, Polli JW, Bourdet DL, Feng B, Huang SM, Liu X, Smith QR, Zhang LK, Zamek-Gliszczyński MJ. Why Clinical Modulation of Efflux Transport at the Human Blood-Brain Barrier Is Unlikely: The ITC Evidence-Based Position. *Clin Pharmacol Ther.* 2013; 94:80–94. [PubMed: 23588303]
40. Polli JW, Baughman TM, Humphreys JE, Jordan KH, Mote AL, Salisbury JA, Tippin TK, Serabjit-Singh CJ. P-glycoprotein influences the brain concentrations of cetirizine (Zyrtec), a second-generation non-sedating antihistamine. *J Pharm Sci.* 2003; 92:2082–2089. [PubMed: 14502547]
41. Kemper EM, Verheij M, Boogerd W, Beijnen JH, van Tellingen O. Improved penetration of docetaxel into the brain by co-administration of inhibitors of P-glycoprotein. *Eur J Cancer.* 2004; 40:1269–1274. [PubMed: 15110893]
42. El Ela AA, Hartter S, Schmitt U, Hiemke C, Spahn-Langguth H, Langguth P. Identification of P-glycoprotein substrates and inhibitors among psychoactive compounds--implications for pharmacokinetics of selected substrates. *J Pharm Pharmacol.* 2004; 56:967–975. [PubMed: 15285840]

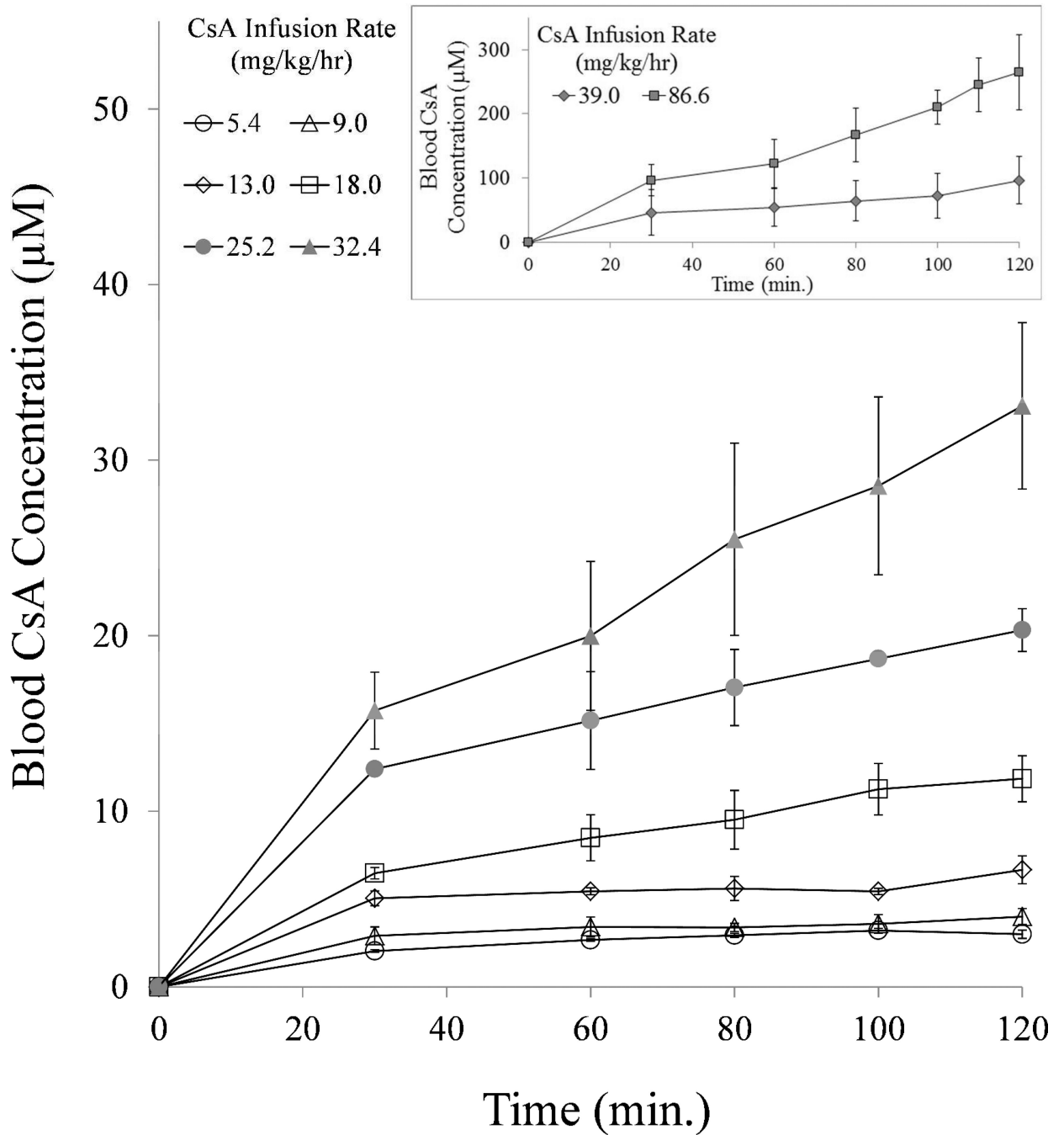


Fig 1.

Except at the higher CsA infusion rates (inset), the expected pseudo steady-state blood CsA concentrations were achieved by 60 min after an i.v. loading dose of CsA followed by an i.v. infusion of CsA.

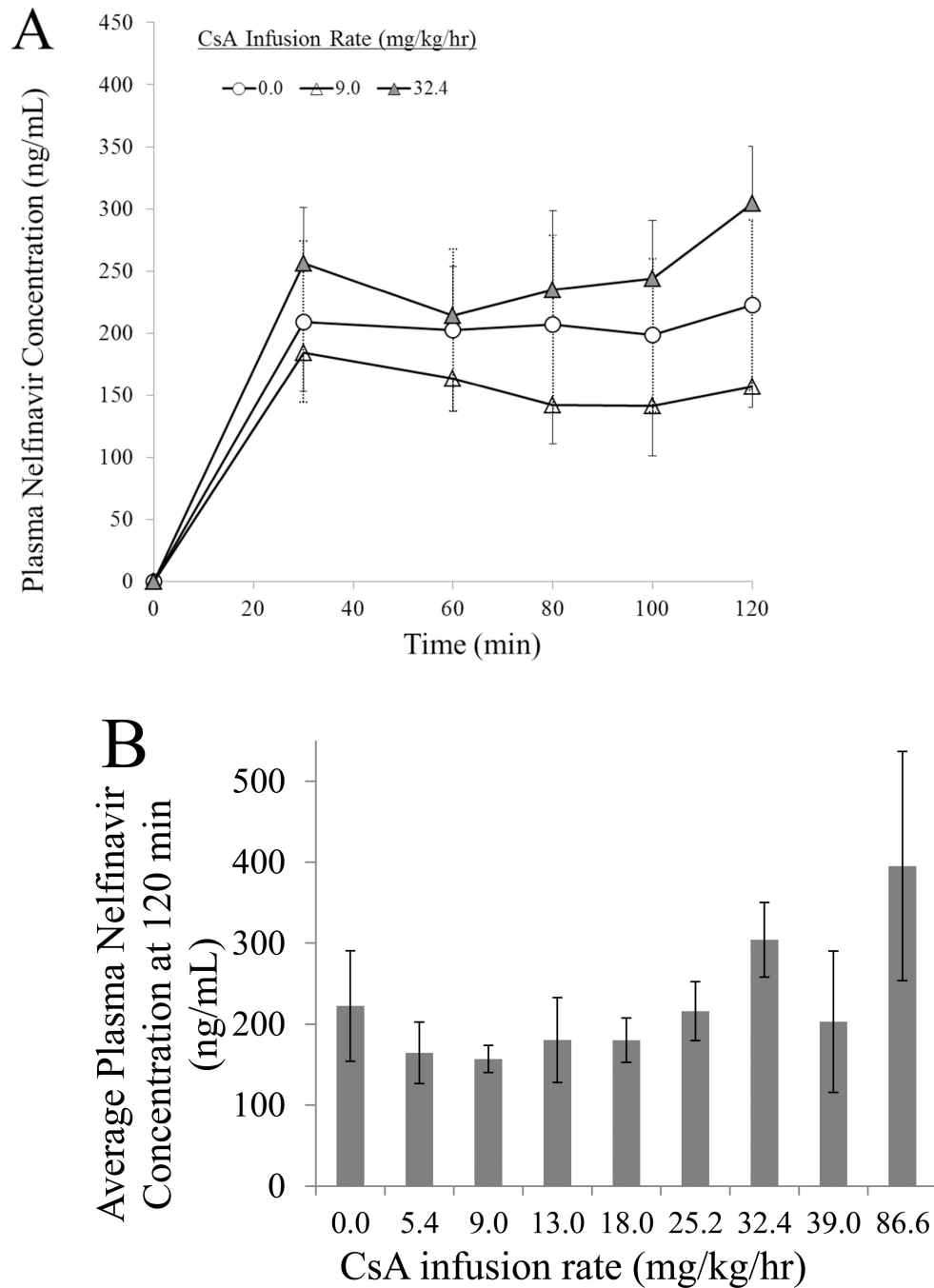


Fig 2. Target NFV plasma concentrations achieved pseudo steady-state by 30 minutes as exemplified by rats that simultaneously received three different rates of CsA infusion; data from all CsA infusion rates are not shown to enhance visual clarity (A). In addition, these target steady-state concentrations (average at 120 min.) were not significantly affected by the presence of CsA (B).

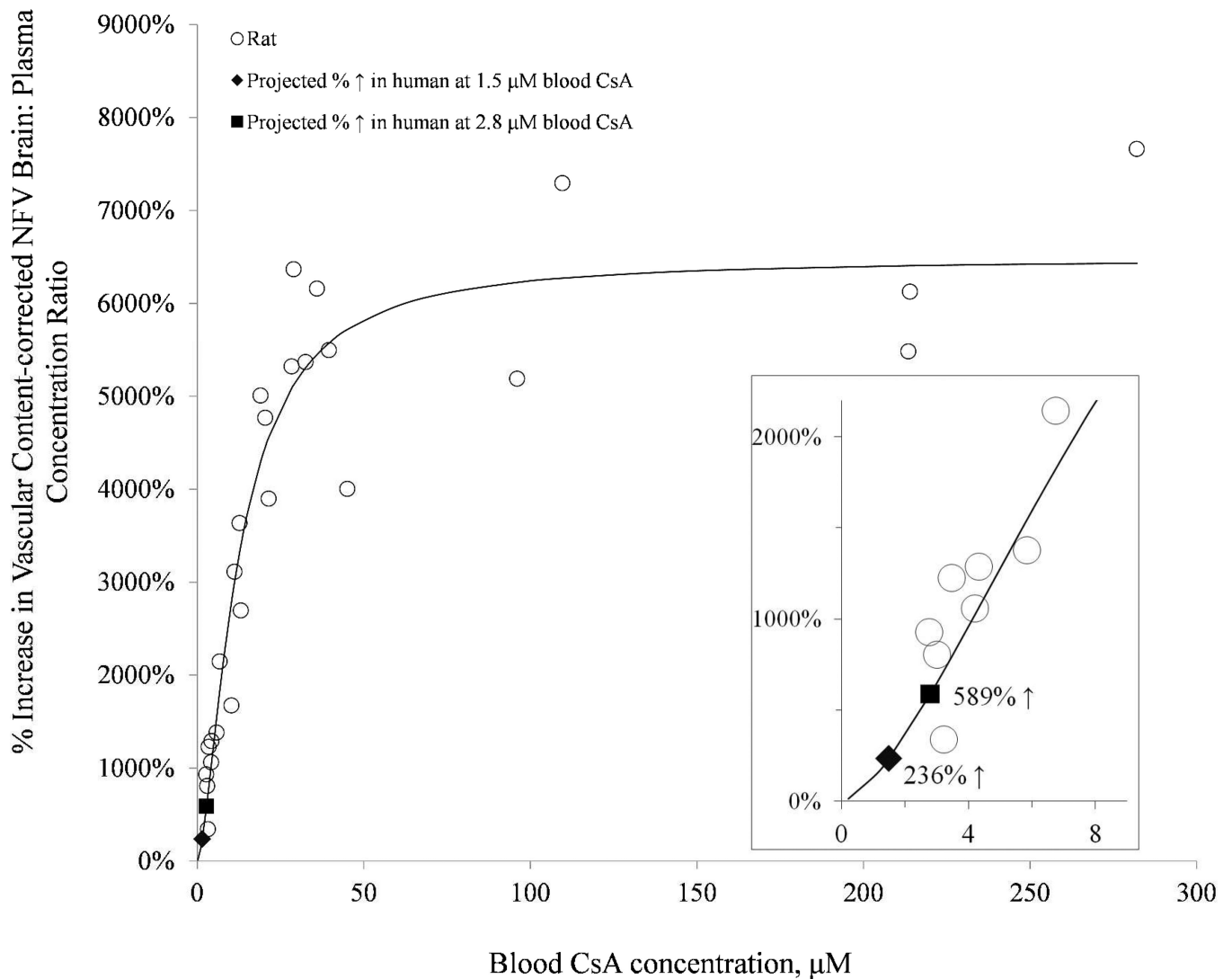


Fig 3.

With increasing CsA blood concentration, the percent increase in the brain:plasma NFV concentration ratio, expressed relative to that in the control group (absence of CsA), increased as the blood CsA concentration increased. The Hill equation was fitted to these data using nonlinear regression (uniform weighting) and yielded the following estimates (% CV of the estimate): E_{\max} 6481% (5.9%), EC_{50} 12.3 μM (13.5%), and γ 1.6 (16.5%). Inset magnifies the lower CsA blood concentration range. At the CsA blood concentration achieved in our prior human PET study (2.8 μM), the fitted model predicted a 589% increase in the NFV brain: plasma concentration ratio (solid square). At therapeutic CsA blood concentration (1.5 μM), the model predicted a 236% increase in the NFV brain: plasma concentration ratio (solid diamond).

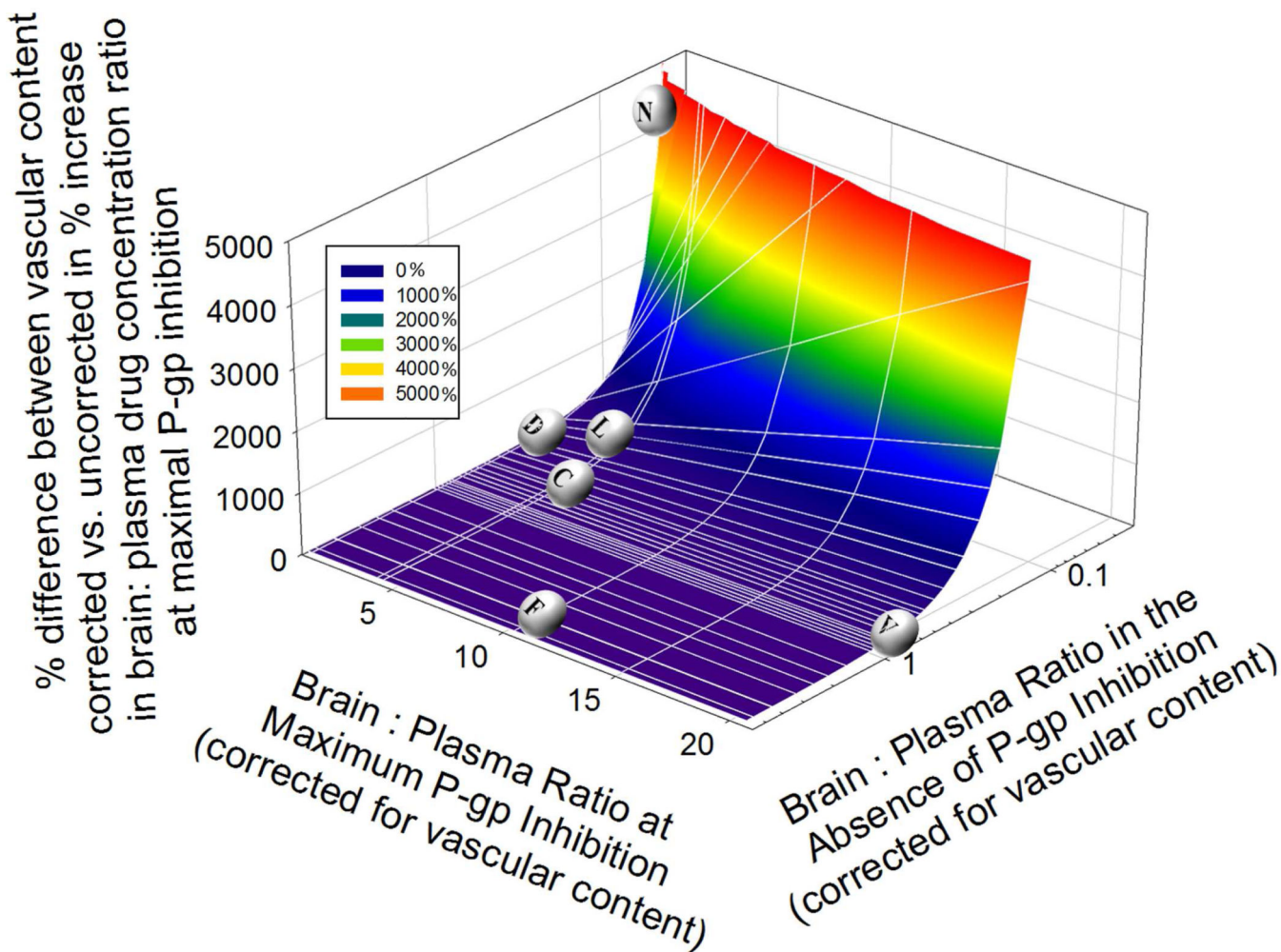
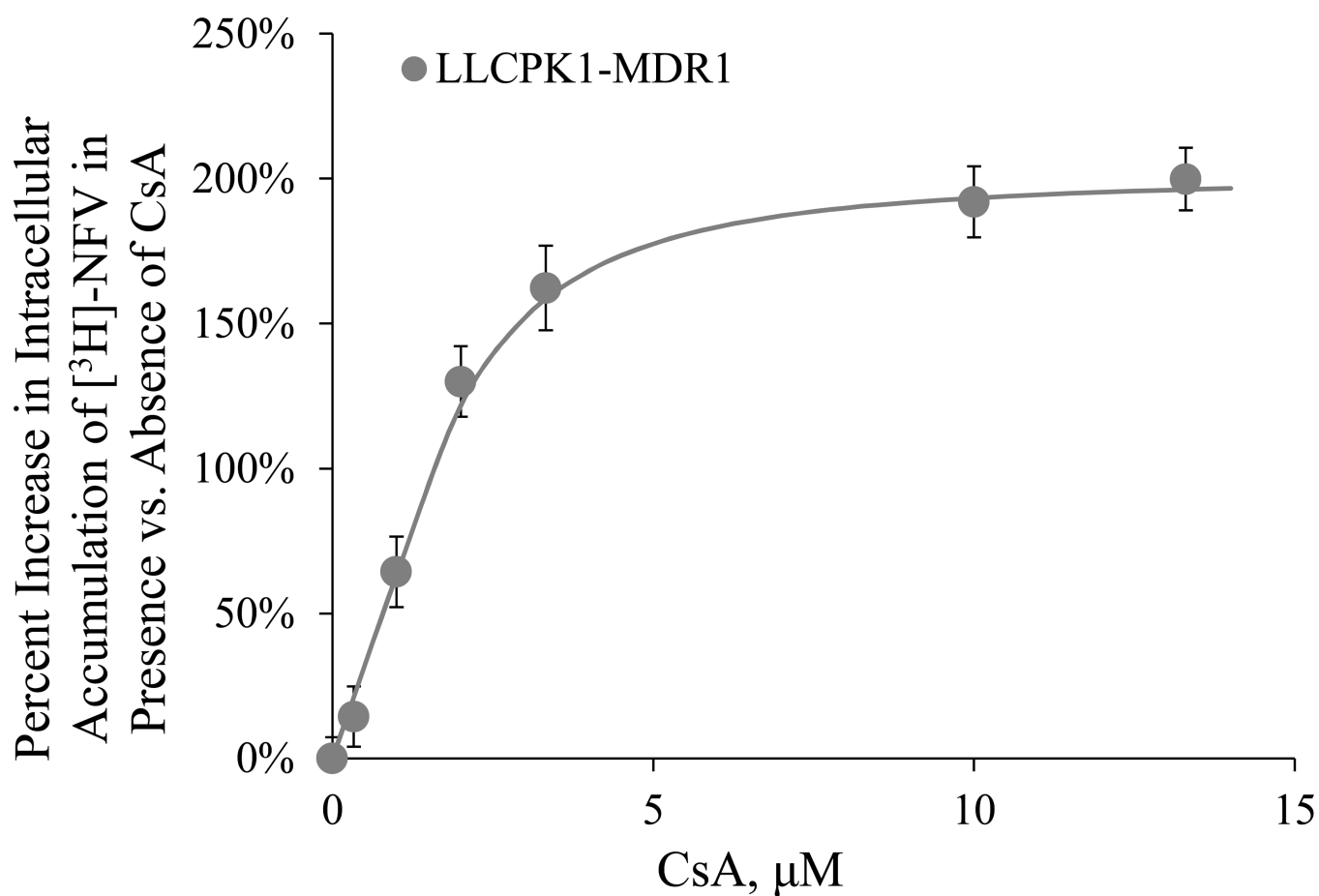


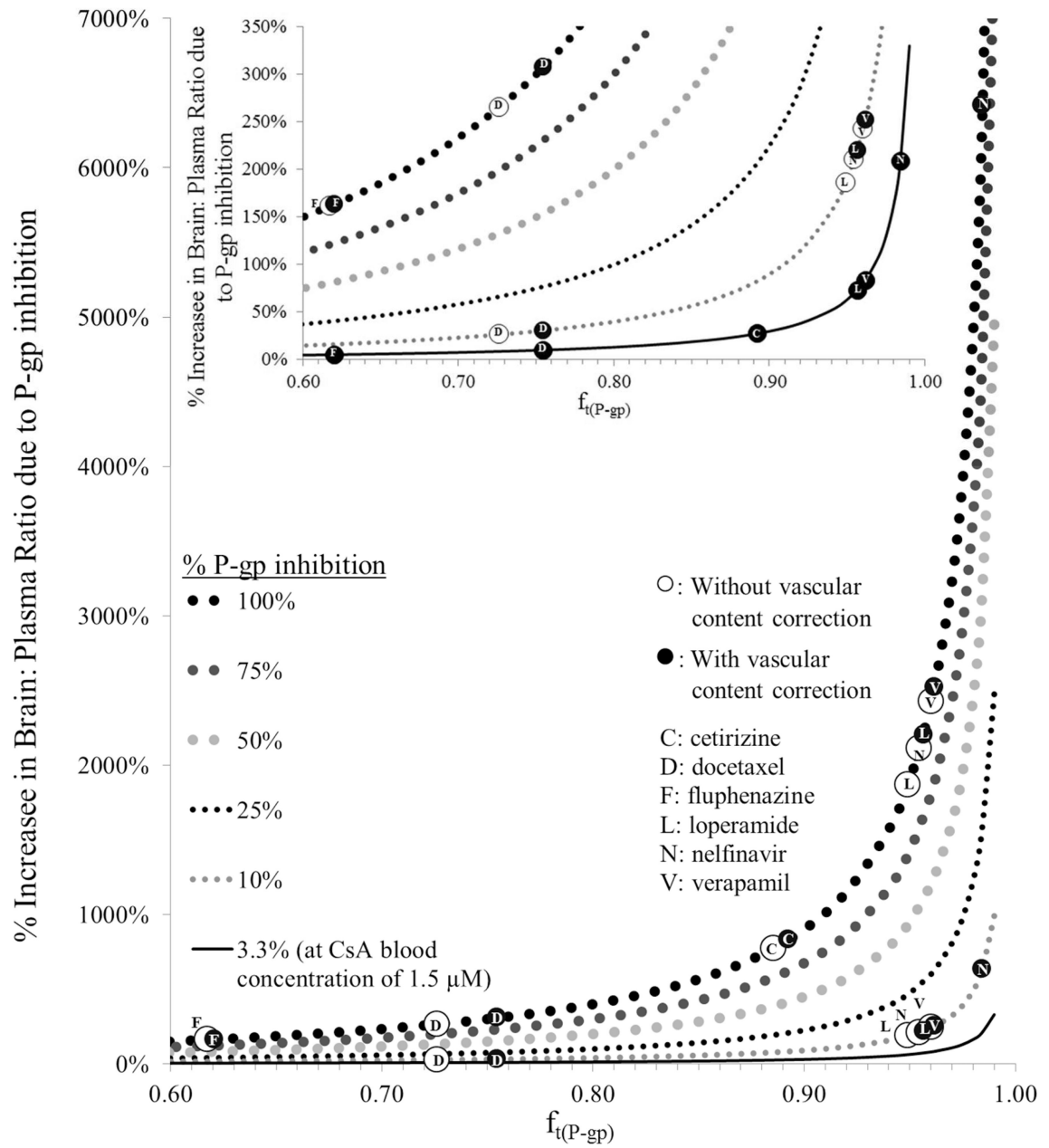
Fig 4.

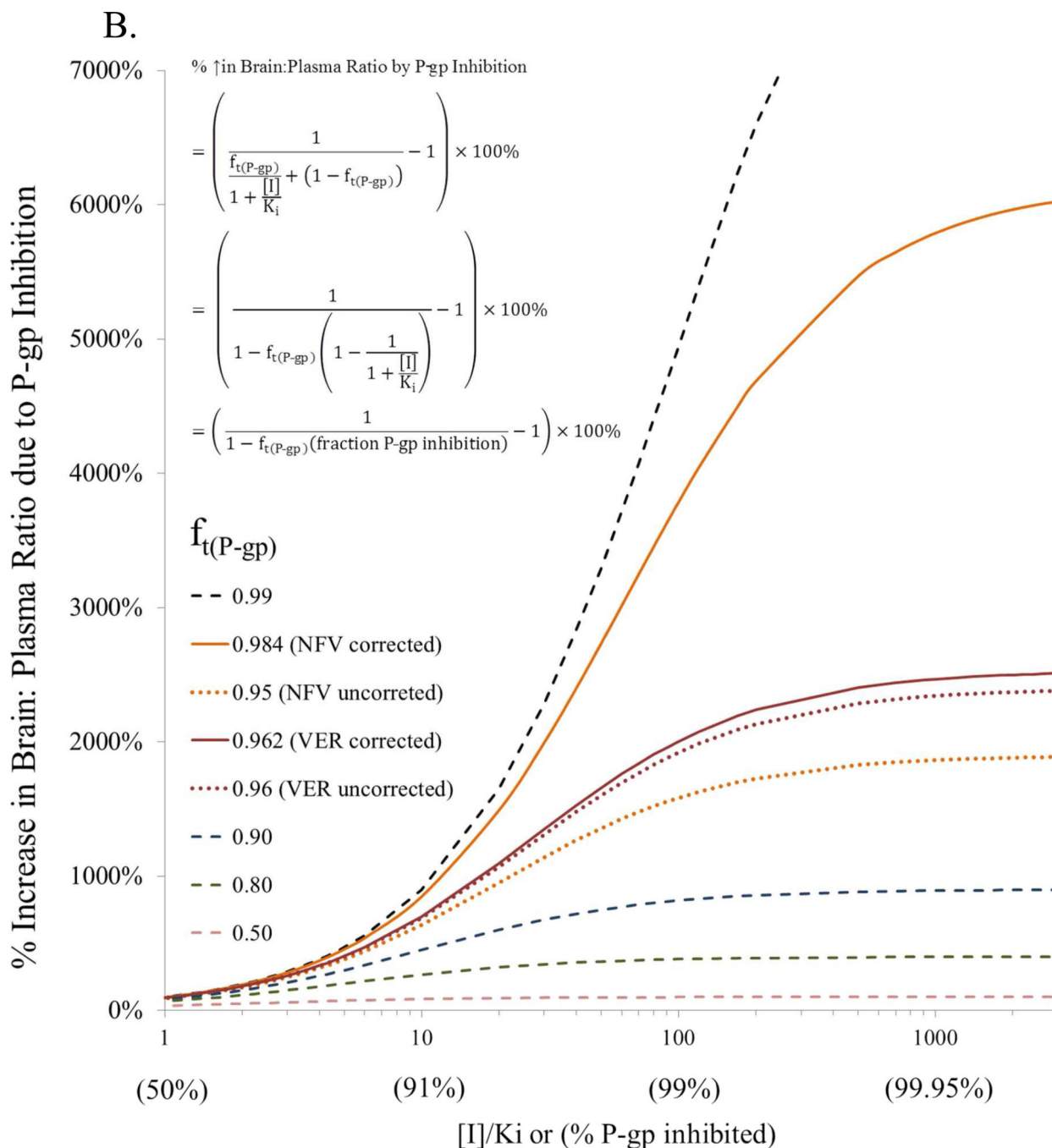
Simulations show the effects of vascular content correction on the % magnitude of maximal P-gp inhibition (corrected versus uncorrected for vascular content contamination). With low brain penetrating P-gp substrates such as NFV (low brain: plasma ratio in the absence of P-gp inhibition), the increase in brain: plasma ratio of the P-gp substrate drug will be considerably underestimated when vascular content correction is not made. As in the case of NFV in this study, at 246.9 μM CsA blood concentration, we reported a 2110% increase in NFV brain: blood ratio without vascular content correction versus 6420% increase when correction is made (differences of 4320%). In contrast, for moderate or high brain penetrating P-gp substrate drugs such as cetirizine (C)⁴⁰, docetaxel (D)⁴¹, fluphenazine (F)⁴², or verapamil (V)¹⁶, on inhibiting P-gp, the % increase in brain: plasma ratio of the drug is relatively unaffected by vascular content correction.

**Fig 5.**

In the LLCPK1-MDR1 cells, the accumulation of intracellular $[^3\text{H}]\text{-NFV}$ increased with increasing CsA concentration. Figure and data shown are based on a representative experiment. In this experiment, increase was described by the Hill equation with an $E_{\text{max}}=187\%$ (2.7%), $EC_{50}=1.56\ \mu\text{M}$ (9.9%), and $\gamma=1.7$ (14%). The values in parenthesis are percent CV of the estimates.

A.



**Fig 6.**

(A) Simulations showing projected maximum % increase in brain: plasma concentration ratio (with and without vascular content correction) when P-gp activity is inhibited versus the fraction of P-gp contribution in the exclusion of the drug from the brain ($f_{t(P-gp)}$) (obtained from studies in rat and mice). As the latter increases, complete inhibition of P-gp can drastically increase the % increase in brain: plasma ratio of the drug (e.g. nelfinavir, N, loperamide, L, verapamil, V – obtained from studies in rats^{16; 18}). The % increase in this ratio is much less for drugs where the contribution of P-gp is lesser ($f_{t(P-gp)} < 97\%$, e.g.

cetirizine, C, docetaxel, D – obtained from studies in mice, fluphenazine, F – obtained from studies in rats) (40, 41, 42) (Inset). In addition, when a drug is efficiently excluded from the brain by P-gp (low brain penetration; $f_{t(P-gp)} > 0.97$) and the drug is highly bound to plasma proteins (where the difference between $f_{t(P-gp)}$ corrected (solid circle) and uncorrected (open circle) is 0.03 or greater, e.g. nelfinavir), if vascular content correction is not made the increase in brain: plasma ratio of the P-gp substrate, on complete inhibition of P-gp, may be considerably underestimated. Simulations also showed projected maximum % increase in brain: plasma concentration ratio for a new molecular entity (NME) at 1.5 μ M blood CsA concentration, when P-gp activity is inhibited by 3.3% (based on CsA EC_{50} of 12.3 μ M and γ of 1.6 from present study) versus the fraction of P-gp contribution in the exclusion of the NME from the brain ($f_{t(P-gp)}$). (B) Using $f_{t(P-gp)}$, and % P-gp inhibition data from (A), plots of % increase in brain: plasma ratio due to P-gp inhibition can be constructed that are comparable to the dependence of the magnitude of drug interaction on f_m (fraction of a dose metabolized via a pathway)^{25; 26; 27}. As $f_{t(P-gp)}$ approaches unity, the % increase in brain: plasma ratio due to P-gp inhibition can be profound when $f_{t(P-gp)}$ is significantly inhibited. Furthermore, for P-gp drug substrate with uncorrected $f_{t(P-gp)} > 0.95$ and difference of $f_{t(P-gp)}$ uncorrected and corrected is 0.03 or greater, the increase in brain: plasma ratio of the P-gp substrate, on complete inhibition of P-gp, may be considerably underestimated (e.g. NFV).